CONF-921117--5

WSRC-MS-92-138

ORIENTATION DEPENDENCY OF MECHANICAL PROPERTIES OF 1950'S VINTAGE TYPE 304 STAINLESS STEEL WELDMENT COMPONENTS BEFORE AND AFTER LOW TEMPERATURE NEUTRON IRRADIATION

by

R.L. Sindelar and G.R. Caskey Jr.

Westinghouse Savannah River Company
Savannah River Technology Center
Aiken, South Carolina 29808

WSRC-MS--92-138

DE93 005168

A paper proposed for publication in the proceedings of the 1st International Symposium on Microstructures and Mechanical Properties of Aging Materials at the TMS-ASM Fall Meeting, in Chicago, IL, November1992 sponsored by the TMS-ASM Mechanical Metallurgy, and Flow and Fracture Committees.

DISCLAIMER

ORIENTATION DEPENDENCY OF MECHANICAL PROPERTIES OF 1950'S VINTAGE TYPE 304 STAINLESS STEEL WELDMENT COMPONENTS BEFORE AND AFTER LOW TEMPERATURE NEUTRON IRRADIATION

by

R.L. Sindelar and G.R. Caskey Jr.

Westinghouse Savannah River Company
Savannah River Technology Center
Aiken, South Carolina 29802

Abstract

Databases of mechanical properties for both the piping and reactor vessels at the Savannah River Site (SRS) were developed from weldment components (base, weld, and weld heat-affected-zone (HAZ)) of archival piping specimens in the unirradiated and irradiated conditions. Tensile, Charpy V-notch (CVN), and Compact Tension C(T) specimens were tested at 25 and 125°C before and after irradiation at low temperatures (90 to 150°C) to levels of 0.065 to 2.1 dpa. Irradiation hardened the weldment components and reduced the absorbed energy and toughness properties from the unirradiated values. A marked difference in the Charpy V-notch absorbed energy and the elastic-plastic fracture toughness (J_{IC}) was observed for both the base and HAZ components with the C-L orientation being lower in toughness than the L-C orientation in both the unirradiated and irradiated conditions. Fracture surface examination of the base and HAZ components of unirradiated C(T) specimens showed a "channel" morphology in the fracture surfaces of the C-L specimens, whereas equiaxed ductile rupture occurred in the L-C specimens. Chromium carbide precipitation in the HAZ component reduced the fracture toughness of the C-L and L-C specimens compared to the respective base component C-L and L-C specimens. Optical metallography of the piping materials showed stringers of second phase particles parallel to the rolling direction along with a banding or modulation in the microchemistry perpendicular to the pipe axis or rolling direction of the plate material.

Introduction

The production reactors at the Savannah River Site (SRS) were constructed and began operation in the 1950's. The service life evaluation of the reactor primary coolant piping system and reactor vessels has been performed by determining the structural integrity of the pressure boundary which is constructed entirely of Type 304 stainless steel. Intergranular Stress Corrosion Cracking is the primary degradation mechanism in sensitized regions of the piping and is a potential degradation mechanism in the vessels. Additionally, the stainless steel sidewalls of the reactor vessels have been exposed to neutron irradiation during reactor operation with nearly all of the fast fluence exposure occurring prior to 1968 when blanketed operation of the core greatly reduced the sidewall exposure rate from the pre-1968 rate. The present maximum dose to the sidewall is 1.4 dpa; the neutron exposure occurred at sidewall temperatures < 130°C [1].

The structural integrity evaluation of the reactor piping and vessels includes evaluation of the impact of postulated flaws on reactor operation. Material properties, especially fracture resistance, for low-temperature irradiated American Iron and Steel Institute (AISI) Type 304 stainless steel weldments (base, weld, and weld heat-affected-zone (HAZ)) are required inputs to flaw evaluation. Mechanical properties for structural and fracture analyses of the piping [2, 3] and reactor vessels [4, 5, 6] were developed in the irradiation and testing of SRS archival Type 304 stainless steel materials.

The unirradiated [2] and irradiated [4] databases for the site piping and vessels included the mechanical test results of Tensile (T), Charpy V-notch (CVN), Compact Tension (C(T)) specimens cut from SRS archival reactor piping and from companion specimens irradiated to 0.065 dpa in the UBR test reactor (Buffalo Materials Research Center) and up to 2.1 dpa in the High Flux Isotope Reactor (HFIR) at Oak Ridge National Laboratory. The mechanical properties were measured at temperatures of 25 and 125°C to bound the range of material temperatures during reactor operation at full power. A comparison of the mechanical response of the weldment components in both the unirradiated and irradiated conditions is presented in this paper. The strong orientation dependency of the toughness of the base and HAZ components (with "low toughness" fracture in the direction of the pipe axis, parallel to the rolling direction of the original plate) is investigated by comparing the features of the microstructure with the fracture surface of the C(T) specimens.

Materials

The original material of construction of the pressure boundary of the reactor primary coolant system including the reactor vessel is 1950's vintage AISI Type 304 stainless steel joined by inert-gas-shielded metal arc welding with Type 308 stainless steel filler wire. The sidewalls of the reactor vessel are constructed from plates 12.7 mm (0.5 in.) thick.

Specimens for the irradiation and mechanical testing studies were cut from eight separate sections of 12.7 mm (0.5 in.) thick archival piping (ASTM A-312-48T (Grade chromium-nickel) with six years of service in the primary coolant system) [7, 8]. Each individual pipe section contained a circumferential butt weld and was referenced to an arbitrarily assigned pipe ring number (1 through 8). The circumferential weld joining the piping was a single Vee; the joint preparation generally contained a small land on the inner diameter (ID) side to aid preweld fitup. The joint was filled from the OD side using several weld passes following a root pass made from the ID side. Mechanical specimens blanks were cut from the piping sections followed by machining to ASTM specifications E8-81 and E21-79 for the T specimens and E23-81, standard size Type A for the CVN specimens. The C(T) specimen design, designated E399 SR is shown in Figure 1. Specimen placement within the original pipe section depended on the weldment component to be tested (see Figure 2) [8]. The T, CVN, and C(T) specimens to test base and weld components were machined to allow the fracture to occur entirely within the respective components. The HAZ component CVN and C(T) specimens in the L-C orientation were machined such that the notch plane was approximately 0.25 inches from the weld fusion line on the piping inside diameter. The corresponding C-L specimens were machined such that the notch root (for CVN) and the precrack depth (for C(T)) were approximately 0.2 inches

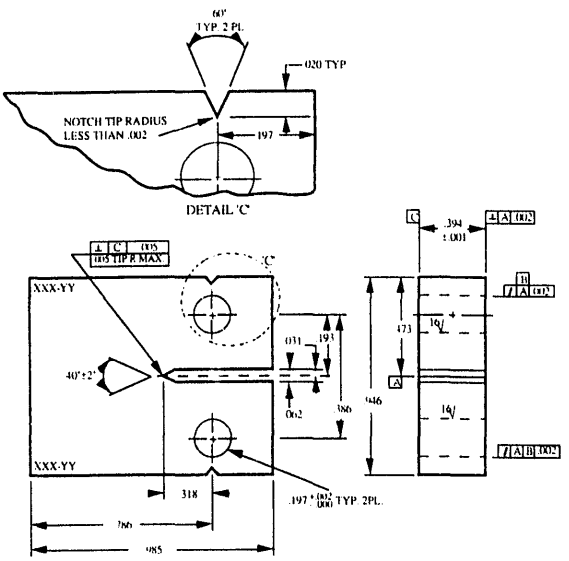

Figure 1: E399 SR 0.4T Compact Tension Specimen Dimensions (inches) [8]. The final specimen design included 20% (10% each side) sidegrooving of the notch plane.

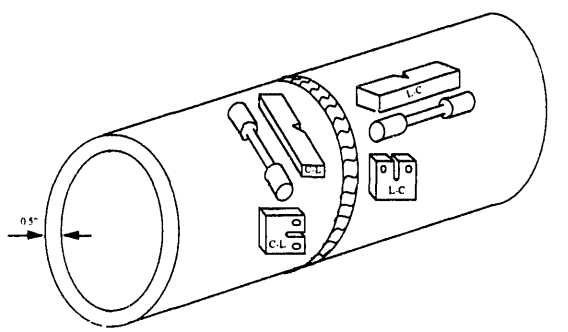

Figure 2: Schematic illustration of specimen orientation in the pipe ring (archival materials [7]). The rolling direction of the original plate used to make the piping is parallel to the pipe axis. The rolling direction of the plate materials used to make the sidewalls of the reactor vessel is along the vessel circumferential direction.

from the weld fusion line on the piping inside diameter. Additional details of specimen placement are contained in reference 8.

The specimens were identified by a material code with the first number of this code signifying the pipe ring number. The adjacent letter indicates the material type (W = weld, B = base, and H = heat-affected-zone or HAZ); the second letter (applicable to base and HAZ material only) identifies the side with respect to the circumferential weld from which the specimen came in the pipe ring (side A or side B) as referenced in the cutting diagrams. A counter number identifying the individual specimen from the particular pipe section was also part of the material code. The chemical compositions of the different base and weld metals for the eight pipe rings are given in Table 1. Delta-ferrite measurements taken along the outer surface of the circumferential weld metal around each of the eight pipe sections show a range of 10 to 15 percent ferrite (Table 2).

Mechanical Testing

The mechanical properties of the base, weld, and weld heat-affected-zone (HAZ) weldment components of the archival piping in the unirradiated and irradiated condition were measured with T, CVN, and C(T) specimens at temperatures including 25 and 125°C [8-10]. The specimens were machined in the ASTM C-L and L-C orientations to allow comparison of the mechanical response for flaws oriented parallel and perpendicular, respectively, to the pipe axis or rolling direction of the original plate. The mechanical results from both the unirradiated archival piping specimens [2, 3] and archival piping specimens irradiated up to 2.1 dpa at temperatures ≤ 155°C [4, 5] show the fracture resistance to be lower in the C-L orientation compared to the L-C orientation; no orientation effects are observed, however, in the tensile test results. The mechanical testing results from the archival piping materials are summarized below.

Irradiation Conditions

Two separate irradiations of the archival piping materials were conducted. A low fluence or Screening Irradiation was performed in the State University of New York at Buffalo Reactor (UBR) and a high fluence or Full-Term Irradiation was performed in the Removable Beryllium position in the High Flux Isotope Reactor (HFIR) at Oak Ridge National Laboratory.

The UBR is a 2 MW light-water-cooled and moderated reactor located in the Buffalo Materials Research facility. A total of 81 CVN and 12 T specimens [6, 8] contained in three independently temperature-controlled capsules forming one irradiation assembly. All of the UBR specimens were irradiated to a nominal thermal and fast fluences of 1.1×10^{19} n/cm^2 and 1.1×10^{20} n/cm^2 ($E_n > 0.1$ MeV), respectively, resulting in a displacement damage level of 0.065 dpa [6, 8]. Thermocouples welded to specimen midsections monitored temperature. The target temperature for each capsule was 120°C ± 15°C. Actual minimum and maximum thermocouple readings from twenty-two thermocouples were 113 and 132°C, respectively. Additional details of the Screening Irradiation are contained in reference 8.

The HFIR is a 85 MW (100 MW prior to November 1986) pressurized light water research reactor at the Oak Ridge National Laboratory. The HFIR Full-Term Irradiation was developed [11] to provide irradiated mechanical property data applicable to the SRS reactor vessel sidewall maximum conditions throughout service life. The Savannah River HFIR irradiation program included four separate capsules, three containing mechanical specimens and one with corrosion specimens. The 1Q capsule, a prototype for the archival piping mechanical specimen capsules, was instrumented with thermocouples and dosimeters to characterize the irradiation conditions in the capsules. Temperatures were measured at the middle and surface of the T, CVN, and C(T) specimens at each end of the capsule and at capsule mid-plane. The temperature ranges were 60 to 100°C for the T specimens, 80 to 140°C for the CVN specimens, and 100 to 155°C for the CT specimens. A total of five T, five CVN, and ten C(T) archival piping specimens were irradiated to doses of 1.0 to 2.1 dpa in the HFIR 4M and tested at 125°C following irradiation. The thermal fluences were 6.2 to 13.1×10^{21} n/cm^2 and the fast fluences were 1.8 to 3.8×10^{21} n/cm^2 ($E_n > 0.1$ MeV). Additional details of the specimen irradiation and testing are provided in references 4 and 5.

Charpy Impact and Tensile Testing

The CVN specimen dimensions conform with those of the standard size Type-A specimen identified in ASTM E 23-81, "Standard Methods for Notch Bar Impact Testing of Metallic Materials." The tensile test specimen gage dimensions conform to ASTM standards E8-81 and E21-79.

Table 1: Base metal chemical compositions (wt%) for archival pipe [1985 chemical analysis]

		Composition (wt-%)										
		C	Mn	Si	P	S	Ni	Cr	Mo	B	Co	Cu	N
1	A	0.079	1.60	0.79	0.031	0.011	9.36	18.79	0.41	0.001	0.11	0.29	0.047
	B	0.035	1.56	0.58	0.024	0.016	9.19	18.44	0.25	0.002	0.10	0.24	0.036
2	A	0.079	1.50	0.34	0.031	0.024	9.65	18.27	0.45	0.002	0.13	0.42	0.043
	B	0.052	1.41	0.38	0.031	0.025	8.50	19.40	0.39	<0.001	0.15	0.42	0.036
3	A	0.063	1.30	0.31	0.028	0.024	9.38	18.59	0.40	0.001	0.12	0.38	0.044
	B	0.048	1.33	0.39	0.027	0.025	9.13	18.67	0.36	0.002	0.13	0.39	0.034
4	A	0.053	1.81	0.33	0.026	0.017	8.75	18.97	0.35	0.002	0.11	0.28	0.033
	B	0.083	1.75	0.74	0.033	0.017	9.60	18.88	0.46	0.002	0.13	0.32	0.043
5	A	0.041	1.39	0.67	0.026	0.024	9.64	19.05	0.52	0.002	0.12	0.28	0.035
	B	0.080	1.25	0.32	0.026	0.016	10.0	18.88	0.44	0.001	0.13	0.41	0.043
6	A	0.058	1.44	0.49	0.027	0.017	9.65	19.05	0.43	0.001	0.15	0.62	0.044
	B	0.046	1.46	0.66	0.026	0.024	8.48	18.88	0.22	0.001	0.13	0.17	0.034
7	A	0.052	1.30	0.55	0.028	0.016	9.35	18.65	0.38	0.002	0.12	0.26	0.039
	B	0.047	1.33	0.34	0.027	0.019	9.15	18.50	0.21	0.001	0.08	0.20	0.037
8	A	0.055	1.30	0.40	0.030	0.026	8.72	19.05	0.42	0.002	0.16	0.45	0.036
	B	0.078	1.75	0.40	0.033	0.018	8.30	19.66	0.44	0.003	0.54	0.34	0.043

Table 1 (cont'd): Weld metal chemical compositions (wt%) for archival pipe

	Composition (wt-%)										
	C	Mn	Si	P	S	Ni	Cr	Mo	B	Co	Cu
1	0.038	1.39	0.41	0.023	0.018	9.65	20.15	0.23	0.002	0.11 0.11[a]	0.21 0.20[a]
2	0.052	1.45	0.41	0.022	0.019	10.50	19.20	0.20	0.005	0.10	0.22
3	0.039	1.25	0.39	0.020	0.017	10.16	19.56	0.21	0.004	0.20	0.21
4	0.047	1.41	0.43	0.022	0.018	10.75	19.29	0.17	0.005	0.094	0.20
5	0.048	1.52	0.42	0.023	0.010	10.15	19.96	0.26	0.001	0.16 0.17[a]	0.23 0.18[a]
6	0.050	1.56	0.49	0.024 0.022[a]	0.008 0.010[a]	10.12	19.87	0.24	<0.001	0.18	0.19 0.19[a]
7	0.042	1.47	0.43	0.020	0.009	9.88	19.47	0.24	0.003	0.15	0.21
8	0.045	1.52	0.37	0.022	0.018	9.70	20.15	0.21	0.002	0.22	0.18 0.16[a]

a Duplicate Analysis Using Separate Stock

Table 2: Average Ferrite Levels for Weld Material of Archival Pipe

Ring #	Weld Reference	Ferrite (%)
1	2PW216W3	13.6
2	6PW1816W3	10.0
3	4PW16W5	15.0
4	1P1W1316W3	10.7
5	2PW1716W2	11.7
6	3PW1516W5	11.2
7	4PW416W4	14.2
8	2PW216W5	14.3

Compact Tension Testing

The 0.4T C(T) specimens (Figure 1) were machined to a thickness of 0.394 inches (10 mm), the maximum that could be machined from the pipe considering the curvature of the large diameter pipe stock. All specimens were side-grooved (10% on each side or 20% total) to reduce crack tunneling to provide an even crack front. A conventional load cell was used to measure the applied load to the CT specimen during testing. Specimen load-line displacement was measured with an outboard clip gage. Crack extension was calibrated with single-specimen compliance techniques and rotation corrections were applied. J-integral resistance (J-R) curve analysis was performed for both the deformation-J (J_D) and modified-J (J_M) methods from the load versus crack extension data. Flow stress values, $s_f = (s_y + s_u)/2$ where s_y and s_u are the yield (0.2% offset) and ultimate tensile strengths, respectively, were obtained from corresponding tensile data or from estimated flow stress properties in the cases where no corresponding data existed. The blunting line is given by $J = 2*(s_f)*\Delta a$. A power-law of the form $J = C(\Delta a^n)$ was fit to the data between the exclusion lines (ASTM E813-81) with the power law toughness corresponding to the onset of stable tearing, J_{IC}, defined as the intersection of the power law curve with the 0.15 mm (0.006 in) exclusion line. Values for J_{IC} were also obtained with a linear regression fit of the data between the exclusion lines per standard ASTM E813-81.

Results

The unirradiated [2] and irradiated [4] mechanical properties databases constructed from the archival piping materials involved several experimentation variables including irradiation conditions (temperature, exposure level, exposure rate, and neutron energy spectrum), weldment component (base, weld, or HAZ), chemical composition, orientation, and test conditions (temperature and testing apparatus). From the test parameters of temperature (25 and 125°C), orientation (L-C and C-L), and weldment component (base, weld, and HAZ), twelve different categories of properties are defined in the evaluation of the mechanical response of the archival piping materials in the unirradiated and irradiated conditions. The results from the unirradiated mechanical property testing [2] show no significant effect of chemical composition on the strength or toughness response; similarly, the irradiated property testing [4, 5, 6] show no significant effect of composition on the response of the material to the low temperature neutron irradiation conditions.

The irradiated mechanical property results of the archival piping materials along with the mechanical results of archival reactor vessel and thermal shield materials are shown as a function of exposure level in references 4 and 5. A slight decrease in toughness was shown with exposure from 0.065 to 2.1 dpa. The change in mechanical properties with exposure level for the archival piping specimens irradiated in the UBR (0.065 dpa) and the HFIR (1.0 to 2.1 dpa) are secondary to the orientation effects on the mechanical response and are not addressed in this report.

The average tensile, impact, and elastic-plastic fracture toughness results for the twelve categories defined by weldment component/test temperature/specimen orientation for the specimen testing are contained in Tables 3 through 8. The unirradiated and irradiated properties in these tables were obtained by averaging the combined set of individual specimen results from the unirradiated testing [2] and the UBR and HFIR 4M irradiated specimen testing [4], respectively.

Tensile Results. Tables 3 and 4 contain the average unirradiated and irradiated results from the testing of T specimens from the archival piping. A total of one to seventeen specimens were tested in each category of the unirradiated property results and a statistical analysis of the uncertainty in the sample mean is provided.

The unirradiated and irradiated strengths at the higher test temperature (125 °C) were slightly lower than the corresponding strengths at the lower temperature (25 °C). Ductility as measured by either total elongation or reduction in area showed little temperature dependence. No significant orientation effect on strength or ductility was observed for the L-C and C-L test directions in the unirradiated condition. The strength and ductility results from the irradiated weld component show slightly higher strength and lower ductility in the C-L orientation although there is insufficient data to evaluate the significance of the difference. Hardening due to irradiation is evident in all of the test data except for the strength of the weld metal at 125°C; the data in the weld material categories is solely from the low-exposure UBR irradiation.

Charpy V-Notch Results. Tables 5 and 6 contain the average unirradiated and irradiated results from the testing of CVN specimens from the archival piping. Irradiation reduced the energy absorption under impact loading, for all test temperatures, orientations, and weld components. The average energy absorption exceeded 50 ft-lbs showing a high toughness for all test conditions. All three material types (base, weld, and HAZ) show a temperature dependence with the lower impact energies at 25°C.

The unirradiated impact test results show a difference of 25 to 60% between the absorbed energies for the C-L and L-C for the base and HAZ components. No significant difference between the C-L and L-C results is shown for the weld component. Irradiation did not change the orientation dependency pattern. The irradiated test results also show the C-L orientation to yield lower absorbed energies than the L-C orientation for the base and HAZ components with differences of 27 to 39%.

Compact Tension Results. Tables 7 and 8 contain the average unirradiated and irradiated results from the testing of C(T) specimens from the archival piping. The average reductions in fracture toughness due to irradiation depended on the weldment component. The largest reductions in toughness occurred for the HAZ specimens. The average unirradiated toughness results for the companion specimens (2W132 and 2W164) of the irradiated weld C(T) specimen (2W2, results listed in Table 8) are a J_{IC} of 1880 in-lb/in^2 with a tearing modulus of 249.

The unirradiated test results show a difference of 33 to 84% between the J_{IC} values for the C-L and L-C orientations for the base and HAZ components. No significant difference between the C-L and L-C results is shown for the weld component. Irradiation did not change the orientation dependency pattern. The irradiated test results also show the C-L orientation to yield lower J_{IC} values than the L-C orientation for the base and HAZ components with differences of 59 to 79%.

Table 3: Unirradiated Tensile Results

Material	Test Temperature (°C)	Sample ASTM Orientation	Engineering Yield Strength (ksi)	Engineering Tensile Strength (ksi)	Elongation* (%)	Reduction in Area (%)
Base	25	L-C	38 (±2)**	91 (±3)	88 (±6)	73 (±6)
		C-L	38 (±2)	92 (±3)	85 (±8)	71 (±5)
Base	125	L-C	29 (±2)	70 (±2)	61 (±3)	77 (±1)
		C-L	29 (±2)	71 (±1)	62 (±3)	73 (±1)
HAZ	25	L-C	-	-	-	-
		C-L	51 (±2)	95 (±3)	86 (±2)	71 (±2)
HAZ	125	L-C	-	-	-	-
		C-L	43 (***)	74 (***)	60 (***)	67 (***)
Weld	25	L-C	55 (±6)	90 (±5)	48 (±10)	64 (±8)
		C-L	57 (±8)	90 (±2)	58 (±30)	57 (±22)
Weld	125	L-C	46 (±2)	72 (±2)	37 (±5)	68 (±12)
		C-L	-	-	-	-

*: Gage length = 0.80 inch
**: Number in parentheses is the 95% confidence interval for sample mean
***: High standard deviation of the sample mean due to small sample size

Table 4: Irradiated Tensile Results

Material	Test Temperature (°C)	Sample ASTM Orientation	Engineering Yield (0.2%) Strength (ksi)	Engineering Tensile Strength (ksi)	Total Elongation* (%)	Reduction in Area (%)
Base	25	L-C	-	-	-	-
		C-L	-	-	-	-
Base	125	L-C	72.9 (2)**	85.0	52.6	68.5
		C-L	74.5 (2)	86.4	37.2	73.5
HAZ	25	L-C	-	-	-	-
		C-L	-	-	-	-
HAZ	125	L-C	81.2 (1)	88.6	NR	NR
		C-L	-	-	-	-
Weld	25	L-C	84.8 (4)	104.3	41.0	60.9
		C-L	93.6 (4)	107.2	32.2	52.8
Weld	125	L-C	55.9 (2)	64.6	36.0	72.6
		C-L	60.2 (2)	65.2	32.0	59.3

*: Gage length = 0.8 inch
**: The number in parentheses is the number of specimens in the sample
NR = Not Reported

Notes: 1) Twelve **Weld** T specimens in the L-C and C-L orientations were irradiated in the UBR and tested at 25 or 125°C [6]. Four **Base** specimens and one **HAZ** specimen were irradiated in the HFIR and tested at 125°C.
2) The range of Young's Modulus for the HFIR 4M specimens is 27.3 to 36.1 x 10^6 psi [4].

Table 5: Unirradiated Charpy V-Notch Results

Material	Test Temperature (°C)	Sample ASTM Orientation	Energy Absorption (ft-lbs)	Lateral Expansion (mils)
Base	25	L-C	149 (±7)*	80 (±4)
		C-L	116 (±5)	83 (±5)
Base	125	L-C	229 (±14)	87 (±2)
		C-L	128 (±11)	77 (±2)
HAZ	25	L-C	136 (±8)	80 (±2)
		C-L	95 (±13)	73 (±6)
HAZ	125	L-C	188 (±33)	85 (±3)
		C-L	101 (±12)	81 (±2)
Weld	25	L-C	113 (±7)	84 (±7)
		C-L	118 (±27)	85 (±3)
Weld	125	L-C	158 (±39)	79 (±6)
		C-L	175 (±16)	83 (±2)

*: Number in parentheses is the 95% confidence interval for the sample mean

Table 6: Irradiated Charpy V-Notch Results

Material	Test Temperature (°C)	Sample ASTM Orientation	Energy Absorption (ft-lbs)	Lateral Expansion (mils)
Base	25	L-C	83 (3)*	67
		C-L	63 (3)	50
Base	125	L-C	94 (4)	80
		C-L	71 (4)	66
HAZ	25	L-C	80 (34)	59
		C-L	54 (3)	43
HAZ	125	L-C	84 (4)	66
		C-L	63 (3)	56
Weld	25	L-C	64 (21)	50
		C-L	-	-
Weld	125	L-C	87 (4)	77
		C-L	78 (3)	65

* The number in parentheses is the number of specimens in the sample.
The results for the **Base**, **HAZ**, and **Weld**, L-C and C-L orientations are the average of the properties of eighty-one UBR and five HFIR 4M data. The 25°C results are from UBR data only. Of the five HFIR data at 125°C, one datum each is in the **Base** L-C and C-L and the **Weld** L-C categories; two data are in the **HAZ** L-C category.

Table 7. Unirradiated Fracture Toughness (Deformation-J, Power law fit)

Material	Test Temperature (°C)	Sample ASTM Orientation	J_{IC} - Deformation (in-lb/in^2)	Tearing Modulus (T)
Base	25	L-C	3380 (±450)*	218 (±23)
		C-L	2420 (±170)	186 (±21)
Base	125	L-C	3310 (±310)	254 (±21)
		C-L	1930 (±190)	218 (±17)
HAZ	25	L-C	2840 (±450)	178 (±27)
		C-L	1790 (±300)	151 (±35)
HAZ	125	L-C	3060 (**)	190 (±21)
		C-L	1250 (**)	155 (**)
Weld	25	L-C	2380 (±420)	244 (±48)
		C-L	2280 (**)	181 (**)
Weld	125	L-C	2780 (**)	300 (±70)
		C-L	3070 (**)	253 (±97)

*: Number in parenthesis is the 95% confidence interval of the mean
**: High standard deviation of the sample mean due to small sample size

Table 8: Irradiated Fracture Toughness (Deformation-J, Power law fit)

Material	Test Temperature (°C)	Sample ASTM Orientation	J_{IC} - Deformation (in-lb/in^2)	Tearing Modulus (T)
Base	25	L-C	-	-
		C-L	-	-
Base	125	L-C	1730 (3)*	127
		C-L	942 (2)	70
HAZ	25	L-C	-	-
		C-L	-	-
HAZ	125	L-C	982 (2)	76
		C-L	428 (2)	18
Weld	25	L-C	-	-
		C-L	-	-
Weld	125	L-C	805 (1)	77
		C-L	-	-

* The number in parentheses is the number of specimens in the sample.
The results are the average of the properties of the HFIR 4M data

Optical Examination

Compact Tension specimen 7HA12 (C-L, 125°C test) had the lowest fracture toughness of the unirradiated materials with a J_{IC} of 875 in-lb/in^2 and a tearing modulus of 121 (Jdeformation, power law fit to J-R curve data). The average fracture toughness results from specimens 7HA3 and 7HA4, the corresponding 7HA L-C specimens, are a J_{IC} of 3660 in-lb/in^2 and a tearing modulus of 200. This difference in fracture toughness results between the C-L and L-C specimens was the largest among the unirradiated materials. The broken C(T) remnants from ring 7, side A materials were therefore selected for additional optical metallography and fractography examination.

Optical metallography was performed on the C(T) half remnant of specimen 7HA12. The specimen was polished down to 0.3 μm diamond paste and successively etched with Vilella's Reagent and Glyceregia followed by repetition of the polish and etch sequence as needed to highlight the grain boundaries and second phase particles. Figure 3a shows the a low magnification optical micrograph of the plane for fracture of the 7HA material with a C-L orientation. The microstructure shows stringers of second phase particles with the long axis parallel to the pipe axis or rolling direction of the original plate. In addition, "flow lines" parallel to the rolling direction are observed in the low magnification micrograph. A high magnification optical micrograph highlighting a delta ferrite stringer is shown in Figure 3b. Intergranular chromium carbide precipitation is also visible in Figure 3b.

Characterization of the microstructure was performed per ASTM E1268-88 [12]. The C-L plane of fracture has an oriented microstructure with high-aspect ratio delta ferrite stringers and elongated, aligned discrete particles. The average number of feature interceptions for test lines perpendicular to the pipe axis or rolling direction is 1.88 ± 0.464 features/mm; the average number of feature interceptions for test lines parallel to the rolling direction is 0.500 ± 0.206. The degree of orientation is 0.64. The average spacing or perpendicular distance between the elongated features is 1/1.88 mm or 530 μm. The L-C plane of fracture for the 7HA material does not have an oriented microstructure.

Characterization of the flow line features in the plane of fracture for the 7HA12 specimen was also performed. The flow line features in the microstructure were highlighted with a nitric and hydrochloric acid etch. The average spacing of the flow lines, calculated by the inverse of the number of interceptions of the flow lines per length of test line, is approximately 40 μm. It is noted that the images of the flow line features are diffuse and that some flow line features are more pronounced than others; therefore, quantification of the spacing is approximate.

Fracture Surface Examination of C(T) Specimens

Fractographs of the broken C(T) specimens from the base and HAZ components of the ring 7, side A material for the L-C and C-L orientations are shown in Figures 4a-d. Both the HAZ and base component specimens show a "channel" morphology to the ductile rupture surface for the C-L orientation whereas the L-C orientation exhibits an equiaxed ductile rupture. The channels in the HAZ C-L specimen are slightly more pronounced than the base L-C specimen. The average ridge-to-ridge spacing of the channels in both the base and HAZ C-L specimen fracture surfaces (Figures 4a and 4c) is approximately 90 μm.

Discussion

The strong dependency of fracture toughness on the orientation with respect to the rolling direction of the austenitic stainless steel plate was observed in a recent heat of Type 316LN stainless steel. Mechanical testing of C(T) specimens identical in design to the SR E399 design (Figure 1) were cut from Type 316LN piping materials and tested at Oak Ridge National Laboratory as part of pipe test program [13]. The fracture toughness test resul. for companion specimens of base component specimens, in the L-C and C-L

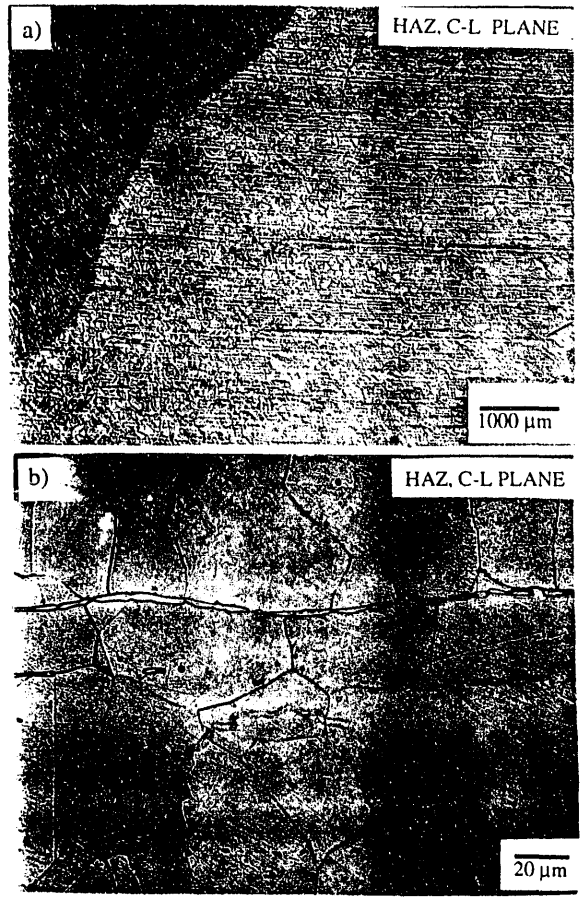

Figure 3: a) Microstructure of the plane of fracture of C(T) specimen 7HA12 (C-L orientation); b) High magnification micrograph of the delta ferrite stringers lying parallel to the pipe axis or rolling direction of the original plate material.

orientations, tested at 110°C, were a J_{IC} of 3040 in-lb/in^2 with a tearing modulus of 163 (L-C orientation) and a J_{IC} of 988 in-lb/in^2 with a tearing modulus of 95 (C-L orientation) [13]. Figures 5a and 5b show flow lines from a plate of Type 316LN stainless steel which was also part of the test program. Flow lines also have been observed in 21Cr-6Ni-9Mn, 19Ni-18Cr, and Type 304L stainless steels and have been shown to correspond to modulation in microchemistry [14, 15]. The location of flow lines observed in both a hot rolled bar and a high energy rate forging of Type 304L stainless steel were shown to correlate to areas enriched in chromium and iron and depleted in nickel by approximately 1 wt.% for each of the respective constituents [15]. It is interesting to note that flow lines were not observed in a hot cross rolled plate of Type 304L stainless steel [15].

The patterns observed in the optical micrographs and on the fracture surfaces of the base and HAZ component specimens of the ring 7, side A material suggest that the weakest fracture path in the microstructure was established during solidification. The nominal dendritic solidification process for a stainless steel of 9.35 % Ni and 18.65 % Cr will tend to develop ferrite and modulations in the Ni/Cr ratio [16]. The extent of these effects will depend on the specific details of the casting process and the location of the material within the ingot - top, bottom, outer surface or interior. As expected, ferrite

stringers and flow lines were not prevalent in every specimen tested in this study, although all specimens were of similar composition. Ordinarily, the times and temperatures encountered in thermomechanical processing are not sufficient to homogenize the microstructures formed during solidification. Consequently, the thermomechanical processing of the steel to form the pipe leads to an oriented pattern of ferrite stringers and flow lines such as those seen in the micrographs. These features are reflected in the elongated "channel-like" dimples observed on the fracture surfaces.

Fracture properties as measured by accepted ASTM methods are markedly more sensitive to orientation and segregation effects than either tensile or impact properties. The data presented here and that reported by Haggag [13] for Type 316LN stainless steel demonstrate a pronounced orientation dependence for fracture properties, especially the elastic-plastic fracture toughness, and with little or no corresponding orientation dependence of the tensile properties. Irradiation of the Type 304 specimens up to 2 dpa at 155 °C did not alter the effect of orientation on the fracture toughness response. This is expected as the irradiation conditions of time, temperature, and dpa do not cause long range rearrangement of the microchemical and microstructural features in Type 304 stainless steel.

Conclusions

The mechanical test results from unirradiated and low-temperature (≤ 160°C), neutron-irradiated (up to 2.1 dpa) specimens from SRS archival Type 304 stainless steel piping materials has shown a strong orientation effect on toughness for base and HAZ weldment components. The C-L orientation exhibits lower Charpy V-notch absorbed energies and elastic-plastic fracture toughness (J_{IC} and T) than corresponding results from L-C specimens. Irradiation did not alter the dependency pattern although the levels of absorbed energy and elastic-plastic toughness were reduced by the irradiation. Strength and ductility results from the tensile specimens did not show a dependency on orientation.

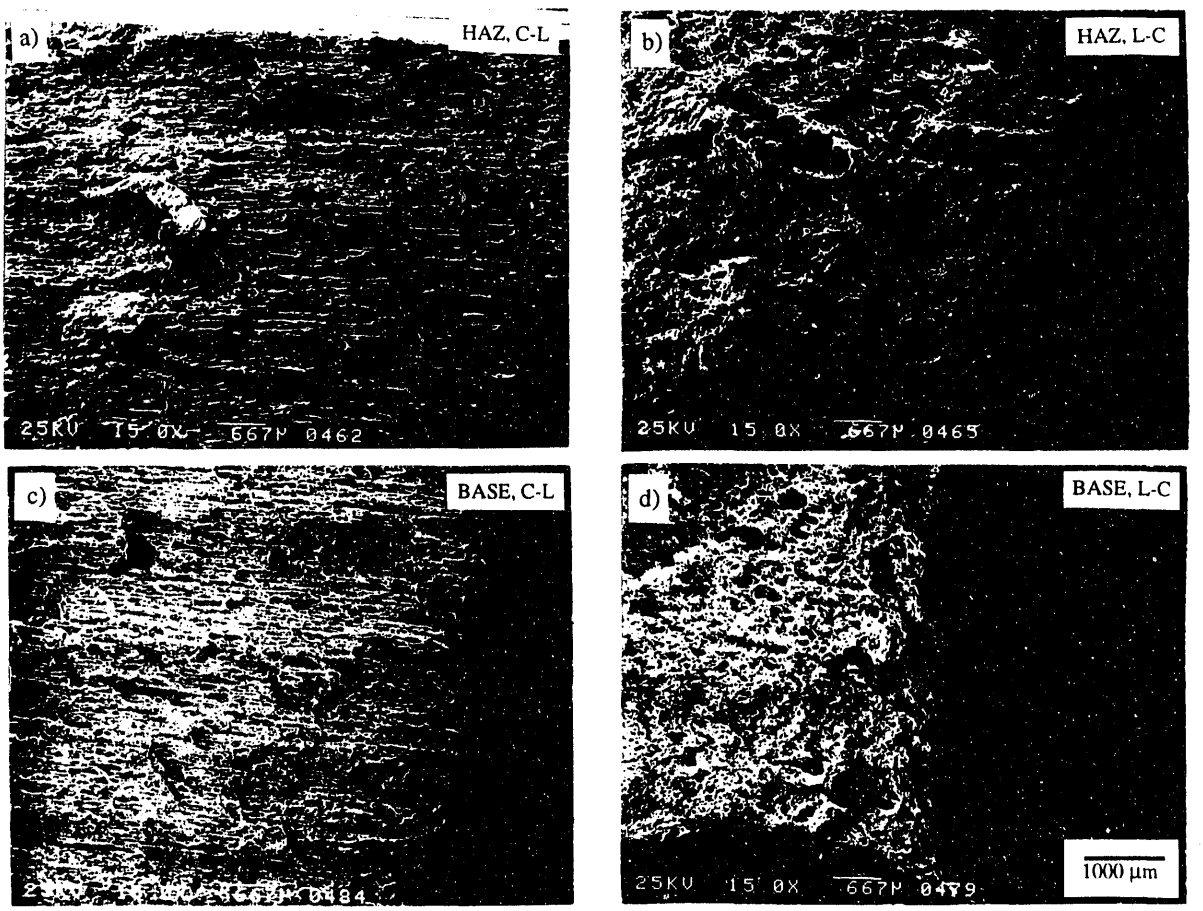

Figure 4: Fractographs of broken C(T) specimens cut from SRS archival piping ring 7, base and HAZ components: a) Specimen 7HA12; b) 7HA4; c) 7BA15S; and d) 7BA18S.

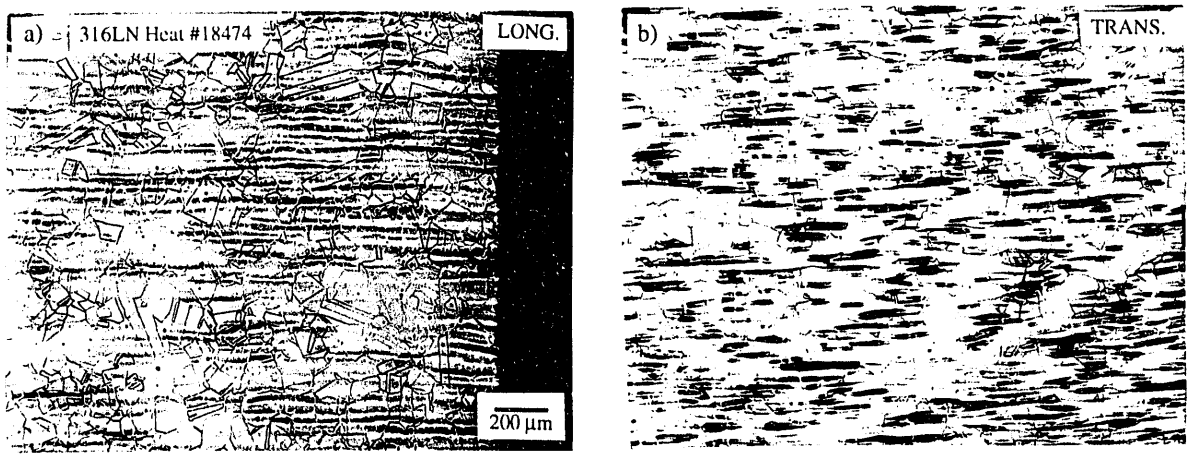

Figure 5: Optical micrographs of Type 316LN stainless steel (reference heat #18474) illustrating flow lines on the planes perpendicular to the plate surface a) in the longitudinal direction, parallel to the rolling direction of the plate; and b) in the transverse direction, perpendicular to the rolling direction of the plate.

Fracture surface examination of unirradiated base and HAZ C(T) specimens for both the C-L and L-C orientations showed full ductile tearing. The morphology of the fracture surfaces of the C-L specimens shows a "channel" morphology whereas the L-C fracture surface is equiaxed dimple rupture. The channel fracture morphology is consistent with the orientation of the flow lines or modulation in microchemistry and second phase constituents in the microstructure. The strong dependency of fracture toughness on orientation is not limited to the archival SRS piping materials and was observed in a recent heat of Type 316LN stainless steel.

Acknowledgments

The information contained in this article was developed during the course of work under Contract No. DE-AC09-89SR18035 with the U.S. Department of Energy. The work of F.E. Odom and J.R. Durden in performing the optical and scanning electron microscopy for this paper is gratefully acknowledged.

References

1. R.L. Sindelar, N.G. Awadalla, N.P. Baumann, and H.S. Mehta, **"Life Extension Approach to the Reactor Vessel of a Nuclear Production Reactor,"** in *Life Assessment and Life Extension of Power Plant Components*, PVP-Vol. 171, American Society of Mechanical Engineers, 1989.

2. K.J. Stoner, R.L. Sindelar, and G.R. Caskey Jr., **"Reactor Materials Program - Baseline Material Property Handbook-Mechanical Properties of 1950's Vintage Stainless Steel Weldment Components (U),"** Westinghouse Savannah River Co. report *WSRC-TR-91-10*, Savannah River Laboratory, April 1991.

3. K.J. Stoner, R.L. Sindelar, N.G. Awadalla, J.R. Hawthorne, A.L. Hiser, and W.H. Cullen, **"Mechanical Properties of 1950's Vintage Type 304 Stainless Steel Weldment Components,"** in *Fatigue, Degradation, and Fracture* PVP-Vol. 195, American Society of Mechanical Engineers, 1990.

4. R.L. Sindelar and G.R. Caskey Jr., **"Reactor Materials Program - Mechanical Properties of Irradiated Types 304 and 304L Stainless Steel Weldment Components (U),"** Westinghouse Savannah River Co. report *WSRC-TR-91-11*, Savannah River Laboratory, December 1991.

5. R.L. Sindelar, et al. **"Mechanical Properties of 1950's Vintage Type 304 Stainless Steel Weldment Components After Low Temperature Neutron Irradiation,"** presented at the 16th International Symposium on Effects of Radiation on Materials, Denver, CO, June 21-25, 1992, to be published by the American Society for Testing of Materials in a Special Technical Publication.

6. J.R. Hawthorne, B.H. Menke, N.G. Awadalla, and K.R. O'Kula, **"Experimental Assessments of Notch Ductility and Tensile Strength of Stainless Steel Weldments After 120°C Neutron Irradiation,"** *Influence of Radiation on Material Properties: 13th International Symposium (Part II), ASTM STP 956*, F.A. Garner, C.H. Henager, Jr., and N. Igata, Eds., American Society for Testing and Materials, Philadelphia, 1987, pp. 191-206.

7. K.J. Stoner, **"Reactor Materials Program - Materials Source History for Type 304 Stainless Steel Testing Program,"** report *DPST-88-1010*, Savannah River Laboratory, December 1988.

8. J.R. Hawthorne, A.L. Hiser, B.H. Menke, W.H. Cullen and F.J. Loss, **"Sample Preparation, Irradiation, and Testing of 304 Stainless Steel Specimens: Final Report,"** *MEA-2221*, Materials Engineering Associates, Inc., 9700-B Martin Luther King Jr. Highway, Lanham, MD, 20706 for Savannah River Laboratory, August 1987.

9. A.L. Hiser and J.R. Hawthorne, **"Baseline Tests (125°C) of Type 304 Stainless Steel Piping Materials from Project 1101,"** *MEA-2345*, Materials Engineering Associates, Inc. for Savannah River Laboratory, May 1989.

10. J.R. Hawthorne, **"Project 1108 Parametric Study of Fracture Resistance and Welding Variables of Irradiated Type 304 Stainless Steel: Final Report,"** *MEA-2465*, Materials Engineering Associates, Inc. for Savannah River Laboratory, October 1991.

11. K.R. O'Kula, **"Off-site Irradiation Program in Support of the SRP Reactor Service Life Investigation,"** E.I. du Pont, de Nemours, & Co. report *DPST-84-551*, Savannah River Laboratory, June 1984.

12. ASTM E1268-88, *Standard Practice for Assessing the Degree of Banding or Orientation of Microstructures.*

13. F.M. Haggag, Oak Ridge National Laboratory - Metals & Ceramics Division to R.L. Sindelar, private communication of unpublished work, August 1992.

14. M.R. Dietrich, G.R. Caskey Jr., and J.A. Donovan, "J-controlled Crack Growth as an Indicator of Hydrogen-Stainless Steel Compatibility," in *Hydrogen Effects in Metals*, I.M. Bernstein and Anthony W. Thompson, eds., 1981, pp. 637-643.

15. W.C. Mosely Jr., "Flow Lines and Microscopic Elemental Inhomogeneities in Austenitic Stainless Steels," in *Microbeam Analysis-1982*, K.F. J Heinrich, ed., San Francisco Press, 1982, pp. 415-421.

16. **"The Cr-Fe-Ni System,"** *Bulletin of Alloy Phase Diagrams*, 2 (1), (1981) pp. 89-99.

END

DATE FILMED

4/19/93